ACS Medicinal Chemistry Letters 12.3 (2021): 502-507

DOI: https://doi.org/10.1021/acsmedchemlett.1c00045

Peripherally crowded cationic phthalocyanines as efficient photosensitizers for photodynamic therapy

Marie Halaskova,[‡1] Asma Rahali,[‡2,3] Verónica Almeida-Marrero,[2] Miloslav Machacek,[1] Radim Kucera,[1] Bassem Jamoussi,[3] Tomás Torres,*[2,4,5] Veronika Novakova,*[1] Andrés de la Escosura,*[2,4] Petr Zimcik*[1]

[1] Faculty of Pharmacy in Hradec Kralove, Charles University, Ak. Heyrovskeho 1203, 50003, Hradec Kralove, Czech Republic

[2] Universidad Autónoma de Madrid, Calle Francisco Tomás y Valiente, 7, 28049 Madrid, Spain

[3] Didactic research laboratory of Experimental Sciences and Supramolecular chemistry, Faculty of Sciences Bizerte, Carthage University, Zarzouna 7021, Bizerte, Tunisia

[4] Institute for Advanced Research in Chemistry (IAdChem), Campus de Cantoblanco 28049 Madrid, Spain.

[5] IMDEA Nanoscience, Campus de Cantoblanco, 28049 Madrid, Spain.

KEYWORDS: phthalocyanine, singlet oxygen, fluorescence, aggregation, phototoxicity, photodynamic therapy.

ABSTRACT: Photodynamic therapy is a treatment modality of cancer based on the production of cytotoxic species upon the light activation of photosensitizers. Zinc phthalocyanine photosensitizers bearing four or eight peripheral bulky 2-di(pyridin-3-yl)phenoxy substituents were synthesized and pyridyl moieties were methylated to form quaternary nitrogen substituents. The quaternized derivatives did not aggregate at all in water and retained their good photophysical properties. High photodynamic activity was demonstrated on HeLa, MCF-7 and EA.hy926 cells, and the novel phthalocyanines exerted very low EC_{50} ~ 50 nM (for MCF-7 cell line) upon light activation while maintaining low inherent toxicity in the dark (half-maximal toxic concentration, TC_{50} ~ 600 μM), giving thus good phototherapeutic indexes (TC_{50}/EC_{50}) 1409 and 5691. The compounds localized primarily in the lysosomes, leading to their rupture after light activation. This induced an apoptotic cell death pathway with subsequent secondary necrosis as a result of extensive and swift damage to the cells. This work demonstrates the importance of a bulky and rigid arrangement of peripheral substituents in the development of novel photosensitizers.

Cancer is the second leading cause of death globally, accounting for one in six deaths in 2018, and its burdens continue to grow worldwide.[1] The treatment of all cancer types has not yet been solved, making investigations in this area of extraordinary high interest. Photodynamic therapy (PDT) is a modern method of cancer treatment, alternative to surgery or radiation therapy. Its characterized by noninvasive character, possibility of targeting and no serious long-term side effects, which may occur during other cancer treatment modalities.[2-4] PDT uses special drugs, *i.e.*, photosensitizers (PSs), along with excitation light and ubiquitous molecular oxygen to generate singlet oxygen that kills the cancer cells.

Previous studies have shown the great potential of phthalocyanines (Pcs) to become optimal PSs and revealed the basic structure-activity relationships.[5-8] Upon light activation, Pcs are able to transfer energy to molecular oxygen, producing toxic singlet oxygen. They typically absorb light in the optical window of tissues (*i.e.*, 650−850 nm), with high extinction coefficients of over 100 000 $M^{-1}cm^{-1}$. Such light penetrates deeply into tissues, which contrasts to other well-known PSs, *e.g.*, porphyrins, whose main absorption band (Soret band) lies typically at lower wavelengths (~ 400 nm). Bulky substituents on Pcs´ periphery are necessary to hinder undesirable aggregation, which would otherwise lead to loss of photodynamic properties. However, this may not be sufficient in aqueous media, where the π-π interactions between planar and strongly hydrophobic Pc cores are extraordinarily strong. Various surfactants[9, 10] or delivery systems[11-14] have been reported to solve this obstacle, yet these systems may render *in vitro* evaluation and practical use difficult. From this point of view, introduction of bulky charged substituents that suppress aggregation by repulsion forces is the most promising strategy.[15-19] Among charged species, cationic Pcs have been recently demonstrated to possess better *in vitro* PDT efficiencies than the anionic ones.[20, 21] This fact was explained by an effect of environmental pH in cell compartments on Pcs´ ionization, by their different binding to serum proteins, interaction with biomembranes, subcellular localization and relocalization after irradiation.

The motivation of this project was to evaluate how that rigidity of peripheral patterns, their number and charge state (neutral or quaternized) is fundamental for achieving a high PDT efficiency of Pcs. For this purpose, the peripherally crowded Pcs **1**, **1Me**, **2** and **2Me** containing 8 or 16 pyridyl moieties (neutral or quaternized) were designed (Chart 1), synthesized, described from the photophysical point of view, and their photodynamic properties were evaluated in detail through *in vitro* studies. Zinc as a central metal was chosen for its known good coordination stability in the Pc core, for

straightforward synthetic availability and, especially, for increasing singlet oxygen production based on the heavy atom effect.[5, 6, 22-24] Moreover, the selection of compounds was based on the recent positive preliminary results with **2Me**, which was shown to be highly photoactive in the production of reactive oxygen species (ROS) after immobilization on tobacco mosaic virus (TMV) protein crystals, for use as heterogeneous catalysts in continuous-flow oxidation processes.[25]

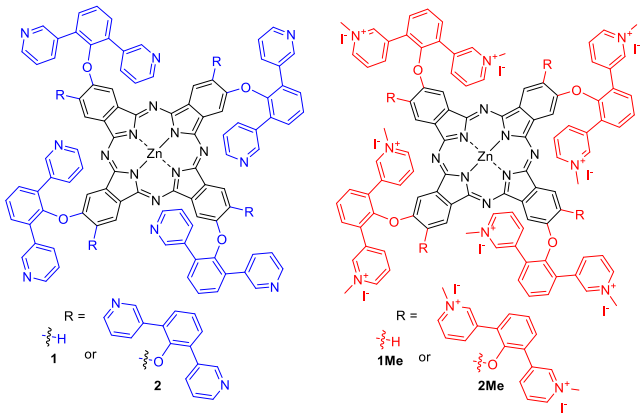

Chart 1: Structures of the target Pcs.

The preparation of tetrasubstituted Pc **1** started with the synthesis of 4-(2,6-di(pyridin-3-yl)phenoxy)phthalonitrile, using (2,6-di(pyridin-3-yl)phenol)[25] and 4-nitrophthalonitrile as precursors, obtaining the product in 71% of yield. Cyclotetramerization of this phthalonitrile in pentanol and with DBU as base, at 140ºC, afforded Pc **1** in 6% yield, which was purified by column chromatography using a mixture of $CHCl_3$/MeOH (10:0.5) with 1% of pyridine, followed by size exclusion chromatography in Biobeads using DCM as eluent. Alkylation of the pyridyloxy groups using methyl iodide in DMF afforded Pc **1Me** in 82% yield (Scheme 1). Pcs **2** and **2Me** were prepared using a previously described procedure.[25] All products were fully characterized by NMR, mass spectrometry, IR and UV-Vis spectroscopy. Importantly, the correlation of intensities between aromatic protons and the N-methyl groups in the ^{1}H-NMR spectrum, together with a clear peak for the molecular ion in the HR-MS spectrum, confirmed the full quaternization of the pyridine moieties in Pcs **1Me** and **2Me**. The purity of the samples was assessed by HPLC and was found to be over 95% for all samples. Additionally, three peaks of positional isomers with different Q-band shapes of absorption spectra were detected during HPLC analysis of **1** (Figure S8), with abundances of 10%, 77% and 11% (the middle peak most likely contained two isomers). However, assignment of the peaks to individual isomers was not possible. The isomers were not separated in **1Me**, but small difference in absorption spectra in ascending, top and descending parts of the chromatographic peak indicated their presence.

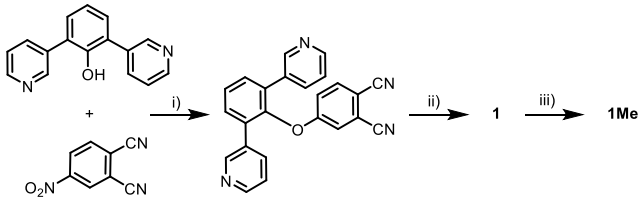

Scheme 1: Synthesis of Pcs **1** and **1Me**. i) K_2CO_3, DMSO, 18 h, 90°C, 71%; ii) $Zn(OAc)_2$, DBU, pentanol, 48 h, 140°C, 6%; iii) CH_3I, DMF, 12 h, 120°C, 82%.

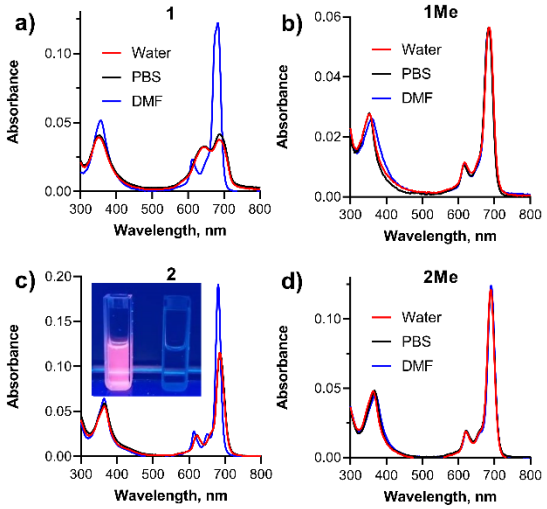

Figure 1. Absorption spectra of compounds **1**, **2**, **1Me** and **2Me** in water (red), PBS (black) and DMF (blue) at 1 μM concentration. The solutions of **1** and **2** were diluted from 100 μM DMSO stock solution. Inset in figure (c) shows the fluorescence of the DMF (left) and PBS (right) solutions (1 μM) of compound **2** (λ_{exc} = 366 nm).

All the prepared Pcs showed absorption spectra in DMF that are typical for monomeric Pcs, with sharp Q-bands over 680 nm and B-bands at approximately 360 nm (Table 1, Figure 1). Evidently, quaternization did not affect the position and the shape of the Q bands. Negligible splitting in the Q-band of **1** was the result of the presence of positional isomers since these Pcs were prepared from monosubstituted phthalonitrile. The splitting was not observed for **1Me** after quaternization. The absorption spectra of non-quaternized Pcs recorded in phosphate-buffered saline (PBS, the same results were obtained in water) differed significantly from those in DMF. A significant decrease of the Q-band intensity and appearance of a new blueshifted band of **1** indicated strong aggregation of this Pc under aqueous conditions (Figure 1a). Although the sharp Q-band of Pc **2**, with only decreased intensity and slight broadening, suggested its presence in the monomeric form, no fluorescence was emitted from the PBS or water solutions (Figure 1c). Similar observations have been reported for extremely bulky phenoxy-substituted Pcs and were ascribed to the formation of atypical aggregates that do not differ from monomers in the shape of the absorption spectrum.[19, 26, 27] The absorption spectra of quaternized Pcs **1Me** and **2Me** in PBS, in turn, were also characteristic of the monomeric form and perfectly overlapped the spectra in DMF. In contrast to Pc **2**, a strong fluorescence emission was preserved this case. The fully monomeric characters of **1Me** and **2Me** in water, which are a crucial prerequisite for obtaining good PDT properties *in vitro*, were further proven spectroscopically based on the accordance of the shape of excitation fluorescence spectra with the corresponding absorption spectra (Figure S13). The shape of the absorption spectra did not change, even at a concentration 100 μM (Figure S13), indicating a very efficient

inhibition of Pc aggregation by this extremely rigid arrangement of quaternized peripheral substituents.

Photophysical properties, especially quantum yields of singlet oxygen production (Φ_Δ), can suggest the impact of the studied Pcs for PDT. Fluorescence emission defined by fluorescence quantum yields (Φ_F) may be used for bioimaging and to localize PSs at the subcellular level or in the tissues. Two different methods have been employed for the determination of both Φ_Δ and Φ_F values in DMF to confirm the accuracy of the obtained data. DMF was a solvent of choice because it ensures good solubility of the whole series, guarantees monomeric character of compounds and provides relevant published value of Φ_Δ of unsubstituted zinc phthalocyanine, used as a reference in the chemical method (see below). The data are summarized in Table 1. The Φ_Δ values were determined with unsubstituted zinc Pc as the reference, using either the chemical method with 1,3-diphenylisobenzofuran as a selective scavenger of singlet oxygen or by the phosphorescence method observing phosphorescence of generated singlet oxygen at 1276 nm (Figure S12). Value of singlet oxygen lifetime (τ_Δ) was about 17 μs for all the samples, which is in accordance to the data published in the literature.[28] All prepared Pcs were characterized by Φ_Δ values 0.49-0.60 in DMF, which is in good agreement with the data previously published for similar zinc Pcs,[18, 19] confirming their monomeric character and indicating the great potential of these derivatives for photodynamic treatments. For the determination of Φ_F value (in DMF and PBS), an absolute method using an integrating sphere and a relative method using zinc Pc as the reference were used. In addition, in this case, the obtained Φ_F values corresponded each other, thus proving the relevance of the measured data. Interestingly, the non-quaternized compounds **1** and **2** possessed higher Φ_F in DMF, close to 0.30, whereas Φ_F values of the corresponding quaternized analogues **1Me** and **2Me** were in the range of 0.16-0.19. The identical values of Φ_F for **1Me** and **2Me** were also determined in PBS, further confirming the monomeric character of **1Me** and **2Me** under aqueous conditions and making the following *in vitro* experiments reasonable. Fluorescence lifetimes (τ_F) ranged 2.17 – 3.15 ns and correlated well with Φ_F values. For **1** and **2**, in turn, no fluorescence was detected in PBS due to aggregation.

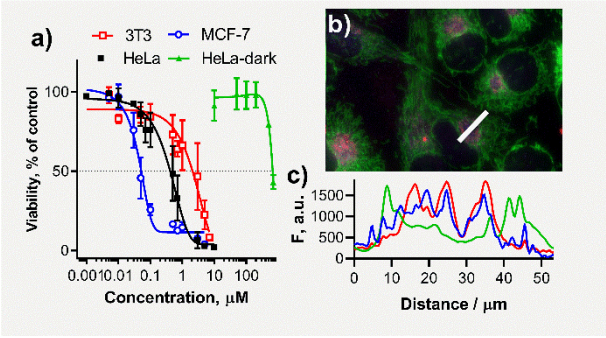

Figure 2. a) Photodynamic activity of compound **1Me** on 3T3 (red), HeLa (black) and MCF-7 (blue) cells (λ > 570 nm, 12.4 mW cm^{-2}, 15 min, 11.2 J cm^{-2}) and dark toxicity of **1Me** on HeLa cells (green). b) Subcellular localization of **1Me** (red) in HeLa cells. Cells were stained for mitochondria (green) and lysosomes (blue) by organelle-specific fluorescent probes. c) The intensity profiles of **1Me** (red), lysosomes (blue) and mitochondria (green) alongside the white bar shown in part b).

All four prepared compounds were subsequently evaluated *in vitro* on the various cell lines - human cervical carcinoma, (HeLa), human breast carcinoma (MCF-7), nonmalignant mouse fibroblasts (3T3) and immortalized human endothelial cells (EA.hy926). Their photodynamic activity after activation by light (λ > 570 nm, 11.2 J cm^{-2}) was expressed as the half-maximal effective concentration (EC_{50}), while inherent toxicity without activation (dark toxicity) was expressed as the half-maximal toxic concentration (TC_{50}), see Figure 2 and S16. The non-quaternized derivatives **1** and **2** precipitated above 1 μM concentration in the cell-culture medium without any detectable toxicity toward HeLa cells either in the dark or upon activation. This is a consequence of the above-discussed tendency toward aggregation in water-based media, leading to inactive forms of PSs, for which these compounds were not evaluated further. Conversely, both quaternized Pcs **1Me** and **2Me** induced concentration-dependent toxicity upon light activation on all cell lines (Table 2). Both Pcs appeared to be most active against MCF-7 cells with EC_{50} values ~ 0.049 μM. Approximately an order of magnitude lower activity was observed against HeLa cells. The results of both Pcs on nonmalignant 3T3 cells differed substantially. While high toxicity was determined for **2Me**, statistically significant lower phototoxicity was observed for **1Me** in comparison with MCF-7 cells (p = 0.049, Welch's t-test). This suggests that **1Me** may have beneficial effect in the PDT treatment, and even after light activation, it may efficiently destroy some types of carcinoma cells while preserving surrounding healthy tissues to some degree. Nevertheless, the results do not exclude **2Me** from further studies since the selectivity in PDT is primarily driven by irradiation of the target areas only. Moreover, this compound exerted much better photoactivity than **1Me** independently of the type of cell line. In comparison with clinically approved PS, both studied compounds appeared to be very efficient; their activity was much higher than for the sulfonated hydroxyaluminium Pc (S_3AlOHPc) that has been approved in clinical practice in Russia under the tradename Photosens®. EC_{50} values determined for S_3AlOHPc by our research group under the identical experimental conditions were higher than 2 μM for all cell lines tested (see Table 2). Photodynamic treatment of HeLa cells using both investigated compounds without any previous incubation, *i.e.*, irradiation started immediately after application of dyes (Figure S17), resulted in EC_{50} values of 1.28 ± 0.68 μM and 0.178 ± 0.024 μM for **1Me** and **2Me**, respectively. Even though a decrease in activity was expected, both compounds proved to maintain their photodynamic activity well. This preservation of photodynamic activity may be utilized in PDT modalities where omission of PS's uptake (or its ample reduction) is conveniently availed (*e.g.*, in vascular-targeted photodynamic therapy). Therefore a similar experiment utilizing human endothelial cells (EA.hy926) was conducted, with comparable results (Table 2). The dark toxicities of both quaternized compounds were low (TC_{50} > 600 μM, Figure 2 and S16 and Table 2) and were either comparable or even lower than those of similar hydrophilic multicationic compounds.[20] Phototherapeutic indicies (*i.e.*, TC_{50}/EC_{50} ratios) revealed very favorable values (HeLa cells) of 1409 and 5691 for **1Me** and **2Me**, respectively.

Active Pcs **1Me** and **2Me** were further studied in detail on HeLa cells. Their uptake after 12 h of incubation reached values 0.26 and 0.50 nmol *per* mg of protein, which are comparable with those of other multicationic Pcs.[20] Uptake of quaternized compounds led to their accumulation in the endo-

lysosomal compartment of HeLa cells, as confirmed by fluorescence microscopy (Figure 2b,c and S14, S15). Unfortunately, both compounds photobleached quickly in the cells. Together with rather rapid re-localization to the cytoplasm, these aspects made **1Me** and **2Me** difficult to image in their primary subcellular localization (endosomes and lysosomes). The entire rapid process of photoactivation with violent burst-like release from lysosomes accompanied by further successive photobleaching is shown in the instructive video of irradiation of HeLa cells treated with **1Me** (Supplementary Material). This boisterous re-localization process with simultaneous oxidative damage to cellular components can lead to cell death. With lysosomes as the primary site of photodynamic damage, irradiation of the cells leads to activation of extrinsic- and intrinsic-pathway initiator caspases 8 and 9, respectively, and executioner caspases 3/7 at the same time, presumably by lysosomal enzyme cleavage of pro-caspases (Figure 3a, S18). Using Annexin V luciferase fusion proteins and a DNA-binding probe allowed for real-time monitoring of cell demise. Exposure of phosphatidylserine, monitored as an increase of luminescence signal, began readily after irradiation, followed by the increase in fluorescence after an apparent lag as a result of the subsequent loss of membrane integrity during secondary necrosis (Figure 3b-e, S19). This lag between inception of the increase in both signals can be used to distinguish between apoptosis followed by secondary necrosis (observed as pronounced delay) and primary necrosis (observed as short or absent delay between increase in luminescence and fluorescence signals).[29] A substantial delay (> 5 h) is observable in apoptosis-positive controls (camptothecin and bortezomib as the inducers of intrinsic pathway-mediated apoptosis (Figure S19) and FasL and TRAIL as the extrinsic pathway inducers (Figure 3e, S19), while both studied compounds displayed evidence of secondary necrosis faster at higher dosages (even within 3.5 h after light activation). Hydrogen peroxide (which is known to induce oxidative damage and necrosis) resulted in initiation of the loss of membrane integrity within half an hour after addition to the cells, which is in accordance with the necrotic type of cell death. Digitonin (necrosis *via* cellular membrane permeabilization) induced devastating non-apoptotic cell death even more rapidly (Figure 3d). Cell death processes after light-induced photodynamic action of **1Me** and **2Me** involves the initial induction of apoptosis, but thanks to extensive and swift damage to the cells by higher dosage of PSs, secondary necrosis might take over even within 3.5 h.

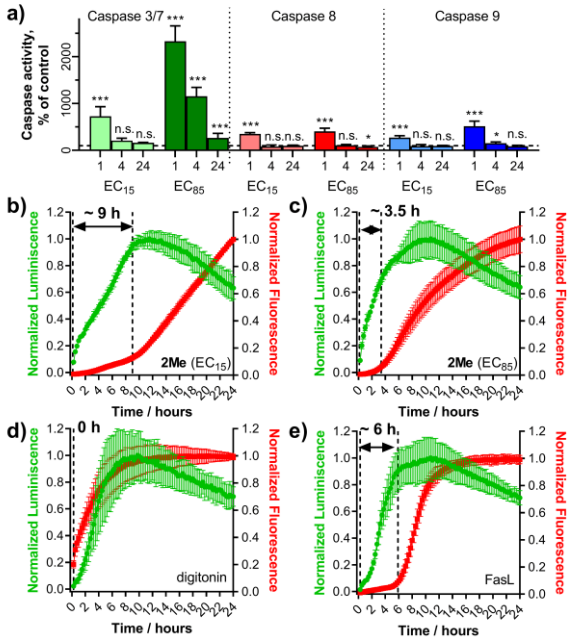

Figure 3. Cell death determinations: a) Caspases 3/7 (green), 8 (red) and 9 (blue) activities for **2Me** in different time after irradiation. b-e) Annexin V (green) and DNA-binding probe (red) binding profiles for **2Me**, at EC_{15} (b) and EC_{85} (c), digitonin (d; necrosis control) and FasL (e; apoptosis control).

In conclusion, this work has demonstrated that an efficient rigid arrangement of peripheral cationic substituents on the aromatic core of Pcs efficiently inhibits aggregation, even in water. This keeps the PS molecules exclusively in a monomolecular state, which is very important for providing good photophysical properties and concomitantly high photodynamic activity. This outcome was demonstrated on cancerous cell lines for the cationic compounds **1Me** and **2Me**, providing much better EC_{50} values than the clinically approved S_3AlOHPc. Further *in vitro* investigation revealed that the main cell demise pathway is through apoptosis with subsequent secondary necrosis after rupture of the lysosomal vesicles, *i.e.*, the organelles of primary subcellular localization. Therefore the concept of introducing charged moieties on the rigid peripheral substituents was confirmed as a highly viable approach for delivering novel, highly active PSs.

ASSOCIATED CONTENT

Supporting Information

The Supporting Information is available free of charge on the ACS Publications website. Synthesis, full characterization of target products, additional absorption spectra, NMR spectra, experimental parts (PDF), video of the photodynamic activity of **1Me** on HeLa cells (mp4).

AUTHOR INFORMATION

Corresponding Author

* E-mails: P. Zimcik: zimcik@faf.cuni.cz, V. Novakova: veronika.novakova@faf.cuni.cz, A. de la Escosura: andres.delaescosura@uam.es, T. Torres: tomas.torres@uam.es

Author Contributions

‡These authors contributed equally.

Notes

The authors declare no competing financial interest.

ACKNOWLEDGMENT

The work was supported by the Czech Science Foundation (19−14758Y), Charles University (PRIMUS/20/SCI/013, GAUK 1620219, SVV 260 550) and by the project EFSA-CDN (No. CZ.02.1.01/0.0/0.0/16_019/0000841) co-funded by the ERDF. For affiliations 2, 4 and 5, the work was supported by MINECO-Feder funds (CTQ2017-85393-P (TT), CTQ-2014-53673-P and CTQ-2017-89539-P (AdlE), PCIN-2017-042/EuroNanoMed2017-191, TEMPEAT (TT)). Affiliation 5 (IMDEA Nanociencia) also acknowledges support from the 'Severo Ochoa' Programme for Centres of Excellence in R&D (MINECO, Grant SEV-2016-0686).

REFERENCES

1. World Heatlh Organization, Cancer. **2018**.
2. Hamblin, M. R., Photodynamic Therapy for Cancer: What's Past is Prologue. *Photochem. Photobiol.* **2020,** *96* (3), 506-516.
3. van Straten, D.; Mashayekhi, V.; de Bruijn, H. S.; Oliveira, S.; Robinson, D. J., Oncologic Photodynamic Therapy: Basic Principles, Current Clinical Status and Future Directions. *Cancers* **2017,** *9* (2), 54.
4. MacDonald, I. J.; Dougherty, T. J., Basic principles of photodynamic therapy. *J. Porphyrin. Phthalocyanines* **2001,** *5* (2), 105-129.
5. Claessens, C. G.; Hahn, U.; Torres, T., Phthalocyanines: From outstanding electronic properties to emerging applications. *Chem. Rec.* **2008,** *8* (2), 75-97.
6. Lo, P. C.; Rodriguez-Morgade, M. S.; Pandey, R. K.; Ng, D. K. P.; Torres, T.; Dumoulin, F., The unique features and promises of phthalocyanines as advanced photosensitisers for photodynamic therapy of cancer. *Chem. Soc. Rev.* **2020,** *49* (4), 1041-1056.
7. Li, X.; Zheng, B. D.; Peng, X. H.; Li, S. Z.; Ying, J. W.; Zhao, Y. Y.; Huang, J. D.; Yoon, J., Phthalocyanines as medicinal photosensitizers: Developments in the last five years. *Coord. Chem. Rev.* **2019,** *379*, 147-160.
8. Wong, R. C. H.; Lo, P. C.; Ng, D. K. P., Stimuli responsive phthalocyanine-based fluorescent probes and photosensitizers. *Coord. Chem. Rev.* **2019,** *379*, 30-46.
9. Lau, J. T. F.; Lo, P.-C.; Jiang, X.-J.; Wang, Q.; Ng, D. K. P., A Dual Activatable Photosensitizer toward Targeted Photodynamic Therapy. *J. Med. Chem.* **2014,** *57* (10), 4088-4097.
10. Chow, S. Y. S.; Lo, P.-C.; Ng, D. K. P., An acid-cleavable phthalocyanine tetramer as an activatable photosensitiser for photodynamic therapy. *Dalton Trans.* **2016,** *45* (33), 13021-13024.
11. Zhen, Z.; Tang, W.; Guo, C.; Chen, H.; Lin, X.; Liu, G.; Fei, B.; Chen, X.; Xu, B.; Xie, J., Ferritin Nanocages To Encapsulate and Deliver Photosensitizers for Efficient Photodynamic Therapy against Cancer. *ACS Nano* **2013,** *7* (8), 6988-6996.
12. Lucky, S. S.; Soo, K. C.; Zhang, Y., Nanoparticles in Photodynamic Therapy. *Chem. Rev.* **2015,** *115* (4), 1990-2042.
13. Almeida-Marrero, V.; van de Winckel, E.; Anaya-Plaza, E.; Torres, T.; de la Escosura, A., Porphyrinoid biohybrid materials as an emerging toolbox for biomedical light management. *Chem. Soc. Rev.* **2018,** *47* (19), 7369-7400.
14. Setaro, F.; Wennink, J. W. H.; Mäkinen, P. I.; Holappa, L.; Trohopoulos, P. N.; Ylä-Herttuala, S.; van Nostrum, C. F.; de la Escosura, A.; Torres, T., Amphiphilic phthalocyanines in polymeric micelles: a supramolecular approach toward efficient third-generation photosensitizers. *J. Mater. Chem., B* **2020,** *8* (2), 282-289.
15. Brilkina, A. A.; Dubasova, L. V.; Sergeeva, E. A.; Pospelov, A. J.; Shilyagina, N. Y.; Shakhova, N. M.; Balalaeva, I. V., Photobiological properties of phthalocyanine photosensitizers Photosens, Holosens and Phthalosens: A comparative in vitro analysis. *J. Photochem. Photobiol., B* **2019,** *191*, 128-134.
16. Venkatramaiah, N.; Pereira, P. M. R.; Almeida Paz, F. A.; Ribeiro, C. A. F.; Fernandes, R.; Tome, J. P. C., Dual functionality of phosphonic-acid-appended phthalocyanines: inhibitors of urokinase plasminogen activator and anticancer photodynamic agents. *Chem. Commun.* **2015,** *51* (85), 15550-15553.
17. Li, X. S.; Ke, M. R.; Zhang, M. F.; Tang, Q. Q.; Zheng, B. Y.; Huang, J. D., A non-aggregated and tumour-associated macrophage-targeted photosensitiser for photodynamic therapy: a novel zinc(II) phthalocyanine containing octa-sulphonates. *Chem. Commun.* **2015,** *51* (22), 4704-4707.
18. Makhseed, S.; Machacek, M.; Alfadly, W.; Tuhl, A.; Vinodh, M.; Simunek, T.; Novakova, V.; Kubat, P.; Rudolf, E.; Zimcik, P., Water-soluble non-aggregating zinc phthalocyanine and in vitro studies for photodynamic therapy. *Chem. Commun.* **2013,** *49* (95), 11149-11151.
19. Ghazal, B.; Machacek, M.; Shalaby, M. A.; Novakova, V.; Zimcik, P.; Makhseed, S., Phthalocyanines and Tetrapyrazinoporphyrazines with Two Cationic Donuts: High Photodynamic Activity as a Result of Rigid Spatial Arrangement of Peripheral Substituents. *J. Med. Chem.* **2017,** *60* (14), 6060-6076.
20. Kollar, J.; Machacek, M.; Halaskova, M.; Lenco, J.; Kucera, R.; Demuth, J.; Rohlickova, M.; Hasonova, K.; Miletin, M.; Novakova, V.; Zimcik, P., Cationic Versus Anionic Phthalocyanines for Photodynamic Therapy: What a Difference the Charge Makes. *J. Med. Chem.* **2020,** *63* (14), 7616-7632.
21. van de Winckel, E.; David, B.; Simoni, M. M.; González-Delgado, J. A.; de la Escosura, A.; Cunha, Â.; Torres, T., Octacationic and axially di-substituted silicon (IV) phthalocyanines for photodynamic inactivation of bacteria. *Dyes Pigm.* **2017,** *145*, 239-245.
22. Novakova, V.; Donzello, M. P.; Ercolani, C.; Zimcik, P.; Stuzhin, P. A., Tetrapyrazinoporphyrazines and their metal derivatives. Part II: Electronic structure, electrochemical, spectral, photophysical and other application related properties. *Coord. Chem. Rev.* **2018,** *361*, 1-73.
23. Anaya-Plaza, E.; Aljarilla, A.; Beaune, G.; Nonappa; Timonen, J. V. I.; de la Escosura, A.; Torres, T.; Kostiainen, M. A., Phthalocyanine–Virus Nanofibers as Heterogeneous Catalysts for Continuous-Flow Photo-Oxidation Processes. *Adv. Mater.* **2019,** *31* (39), 1902582.
24. Makhseed, S.; Tuhl, A.; Samuel, J.; Zimcik, P.; Al-Awadi, N.; Novakova, V., New highly soluble phenoxy-substituted phthalocyanine and azaphthalocyanine derivatives: Synthesis, photochemical and photophysical studies and atypical aggregation behavior. *Dyes Pigm.* **2012,** *95* (2), 351-357.
25. Anaya-Plaza, E.; Joseph, J.; Bauroth, S.; Wagner, M.; Dolle, C.; Sekita, M.; Gröhn, F.; Spiecker, E.; Clark, T.; de la Escosura, A.; Guldi, D. M.; Torres, T., Synergy of Electrostatic and π–π Interactions in the Realization of Nanoscale Artificial Photosynthetic Model Systems. *Angew. Chem., Int. Ed.* **2020,** *59* (42), 18786-18794.
26. Kupcho, K.; Shultz, J.; Hurst, R.; Hartnett, J.; Zhou, W.; Machleidt, T.; Grailer, J.; Worzella, T.; Riss, T.; Lazar, D.; Cali, J. J.; Niles, A., A real-time, bioluminescent annexin V assay for the assessment of apoptosis. *Apoptosis* **2019,** *24* (1), 184-197.
27. Machacek, M.; Demuth, J.; Cermak, P.; Vavreckova, M.; Hruba, L.; Jedlickova, A.; Kubat, P.; Simunek, T.; Novakova, V.; Zimcik, P., Tetra(3,4-pyrido)porphyrazines Caught in the Cationic Cage: Toward Nanomolar Active Photosensitizers. *J. Med. Chem.* **2016,** *59* (20), 9443-9456.

Table 1. Photophysical properties of studied compounds[a]

Cpd.	solvent	λ_A, nm	λ_F, nm	Φ_F (absol/comp)	τ_F, ns	Φ_Δ (phos/chem)	τ_Δ, μs
1	DMF	682	689	0.29/0.25	2.89	0.60/0.59	17.7
1Me	DMF	684	692	0.18/0.17	2.19	0.57/0.51	15.2
	PBS	684	695	0.17/0.19	2.83	-	-
2	DMF	681	687	0.29/0.28	3.15	0.59/0.56	18.7
2Me	DMF	693	701	0.16/0.18	2.17	0.58/0.49	17.4
	PBS	690	700	0.16/0.16	2.34	-	-

[a] absorption maximum (λ_A); emission maximum (λ_F); fluorescence quantum yield (Φ_F) determined either by absolute method (absol) or comparative method (comp) (for the details see Supporting information); singlet oxygen quantum yield (Φ_Δ) determined either by phosphorescence method (phos) or by chemical method (chem) (for the details see Supporting information); fluorescence lifetime (τ_F); singlet oxygen lifetime (τ_Δ). Fluorescence lifetimes (τ_F) were determined using HPL laser (653.9 nm).

Table 2. Comparison of Uptake, Dark Toxicity (TC_{50} Values), and Photodynamic Activity (EC_{50} Values) of Studied Pcs in Different Cell Lines[a]

Cpd.	uptake (nmol *per* mg of protein), HeLa	EC_{50} (μM)					TC_{50} (μM)	TC_{50}/EC_{50}
		HeLa	MCF-7	3T3	EA.hy926[e]	HeLa[e]	HeLa	HeLa
1	-	> 1[b]	-	-	-		> 1[b]	-
1Me	0.26	0.48 ± 0.25	0.050 ± 0.014	2.12 ± 1.4	3.43 ± 0.61	1.28 ± 0.68	675 ± 17	1409
2	-	> 1[b]	-	-	-		> 1[b]	-
2Me	0.50	0.11 ± 0.027	0.047 ± 0.016	0.068 ± 0.029	0.50 ± 0.07	0.18 ± 0.024	601 ± 6	5691
S_3AlOHPc		2.07 ± 0.29[c]	2.04 ± 0.31[d]	2.37 ± 0.63[d]	-		>1500[d]	>725

[a] Data are presented as the TC_{50} or EC_{50} values ± standard deviations. TC_{50}/EC_{50} refers to phototherapeutic index. Irradiation conditions: λ > 570 nm, 12.4 mW cm^{-2}, 15 min, 11.2 J cm^{-2}. At least three independent experiments each in quadruplicate were performed. [b]The compounds precipitated above this concentration; [c]Data from ref.[30]. [d]Data from ref.[20]. [e]without preincubation. The cells were irradiated immediately after application of Pc.

TOC graphic

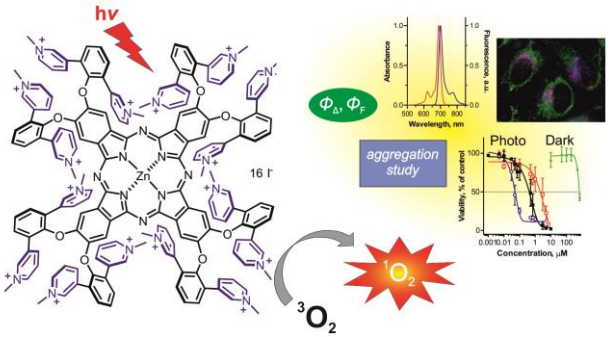

1. World Heatlh Organization, Cancer. **2018**.
2. Hamblin, M. R., Photodynamic Therapy for Cancer: What's Past is Prologue. *Photochemistry and Photobiology* **2020,** *96* (3), 506-516.

3. van Straten, D.; Mashayekhi, V.; de Bruijn, H. S.; Oliveira, S.; Robinson, D. J., Oncologic Photodynamic Therapy: Basic Principles, Current Clinical Status and Future Directions. *Cancers* **2017,** *9* (2), 54.
4. MacDonald, I. J.; Dougherty, T. J., Basic principles of photodynamic therapy. *Journal of Porphyrins and Phthalocyanines* **2001,** *5* (2), 105-129.
5. Claessens, C. G.; Hahn, U.; Torres, T., Phthalocyanines: From outstanding electronic properties to emerging applications. *Chem. Rec.* **2008,** *8* (2), 75-97.
6. Lo, P. C.; Rodriguez-Morgade, M. S.; Pandey, R. K.; Ng, D. K. P.; Torres, T.; Dumoulin, F., The unique features and promises of phthalocyanines as advanced photosensitisers for photodynamic therapy of cancer. *Chemical Society Reviews* **2020,** *49* (4), 1041-1056.
7. Li, X.; Zheng, B. D.; Peng, X. H.; Li, S. Z.; Ying, J. W.; Zhao, Y. Y.; Huang, J. D.; Yoon, J., Phthalocyanines as medicinal photosensitizers: Developments in the last five years. *Coordination Chemistry Reviews* **2019,** *379*, 147-160.
8. Wong, R. C. H.; Lo, P. C.; Ng, D. K. P., Stimuli responsive phthalocyanine-based fluorescent probes and photosensitizers. *Coordination Chemistry Reviews* **2019,** *379*, 30-46.
9. Lau, J. T. F.; Lo, P.-C.; Jiang, X.-J.; Wang, Q.; Ng, D. K. P., A Dual Activatable Photosensitizer toward Targeted Photodynamic Therapy. *Journal of Medicinal Chemistry* **2014,** *57* (10), 4088-4097.
10. Chow, S. Y. S.; Lo, P.-C.; Ng, D. K. P., An acid-cleavable phthalocyanine tetramer as an activatable photosensitiser for photodynamic therapy. *Dalton Transactions* **2016,** *45* (33), 13021-13024.
11. Zhen, Z.; Tang, W.; Guo, C.; Chen, H.; Lin, X.; Liu, G.; Fei, B.; Chen, X.; Xu, B.; Xie, J., Ferritin Nanocages To Encapsulate and Deliver Photosensitizers for Efficient Photodynamic Therapy against Cancer. *ACS Nano* **2013,** *7* (8), 6988-6996.
12. Lucky, S. S.; Soo, K. C.; Zhang, Y., Nanoparticles in Photodynamic Therapy. *Chem. Rev.* **2015,** *115* (4), 1990-2042.
13. Almeida-Marrero, V.; van de Winckel, E.; Anaya-Plaza, E.; Torres, T.; de la Escosura, A., Porphyrinoid biohybrid materials as an emerging toolbox for biomedical light management. *Chemical Society Reviews* **2018,** *47* (19), 7369-7400.
14. Setaro, F.; Wennink, J. W. H.; Mäkinen, P. I.; Holappa, L.; Trohopoulos, P. N.; Ylä-Herttuala, S.; van Nostrum, C. F.; de la Escosura, A.; Torres, T., Amphiphilic phthalocyanines in polymeric micelles: a supramolecular approach toward efficient third-generation photosensitizers. *Journal of Materials Chemistry B* **2020,** *8* (2), 282-289.
15. Brilkina, A. A.; Dubasova, L. V.; Sergeeva, E. A.; Pospelov, A. J.; Shilyagina, N. Y.; Shakhova, N. M.; Balalaeva, I. V., Photobiological properties of phthalocyanine photosensitizers Photosens, Holosens and Phthalosens: A comparative in vitro analysis. *Journal of Photochemistry and Photobiology B-Biology* **2019,** *191*, 128-134.
16. Venkatramaiah, N.; Pereira, P. M. R.; Almeida Paz, F. A.; Ribeiro, C. A. F.; Fernandes, R.; Tome, J. P. C., Dual functionality of phosphonic-acid-appended phthalocyanines: inhibitors of urokinase plasminogen activator and anticancer photodynamic agents. *Chemical Communications* **2015,** *51* (85), 15550-15553.
17. Li, X. S.; Ke, M. R.; Zhang, M. F.; Tang, Q. Q.; Zheng, B. Y.; Huang, J. D., A non-aggregated and tumour-associated macrophage-targeted photosensitiser for photodynamic therapy: a novel zinc(II) phthalocyanine containing octa-sulphonates. *Chemical Communications* **2015,** *51* (22), 4704-4707.
18. Makhseed, S.; Machacek, M.; Alfadly, W.; Tuhl, A.; Vinodh, M.; Simunek, T.; Novakova, V.; Kubat, P.; Rudolf, E.; Zimcik, P., Water-soluble non-aggregating zinc phthalocyanine and in vitro studies for photodynamic therapy. *Chemical Communications* **2013,** *49* (95), 11149-11151.
19. Ghazal, B.; Machacek, M.; Shalaby, M. A.; Novakova, V.; Zimcik, P.; Makhseed, S., Phthalocyanines and Tetrapyrazinoporphyrazines with Two Cationic Donuts: High Photodynamic Activity as a Result of Rigid Spatial Arrangement of Peripheral Substituents. *Journal of Medicinal Chemistry* **2017,** *60* (14), 6060-6076.

20. Kollar, J.; Machacek, M.; Halaskova, M.; Lenco, J.; Kucera, R.; Demuth, J.; Rohlickova, M.; Hasonova, K.; Miletin, M.; Novakova, V.; Zimcik, P., Cationic Versus Anionic Phthalocyanines for Photodynamic Therapy: What a Difference the Charge Makes. *Journal of Medicinal Chemistry* **2020,** *63* (14), 7616-7632.
21. van de Winckel, E.; David, B.; Simoni, M. M.; González-Delgado, J. A.; de la Escosura, A.; Cunha, Â.; Torres, T., Octacationic and axially di-substituted silicon (IV) phthalocyanines for photodynamic inactivation of bacteria. *Dyes and Pigments* **2017,** *145*, 239-245.
22. Novakova, V.; Donzello, M. P.; Ercolani, C.; Zimcik, P.; Stuzhin, P. A., Tetrapyrazinoporphyrazines and their metal derivatives. Part II: Electronic structure, electrochemical, spectral, photophysical and other application related properties. *Coordination Chemistry Reviews* **2018,** *361*, 1-73.
23. Tuhl, A.; Makhseed, S.; Zimcik, P.; Al-Awadi, N.; Novakova, V.; Samuel, J., Heavy metal effects on physicochemical properties of non-aggregated azaphthalocyanine derivatives. *Journal of Porphyrins and Phthalocyanines* **2012,** *16* (7-8), 817-825.
24. Svec, J.; Zimcik, P.; Novakova, L.; Rakitin, O. A.; Amelichev, S. A.; Stuzhin, P. A.; Novakova, V., 1,2,5-Chalcogenadiazole-Annulated Tripyrazinoporphyrazines: Synthesis, Spectral Characteristics, and Influence of the Heavy Atom Effect on Their Photophysical Properties. *European Journal of Organic Chemistry* **2015,** *2015* (3), 596-604.
25. Anaya-Plaza, E.; Aljarilla, A.; Beaune, G.; Nonappa; Timonen, J. V. I.; de la Escosura, A.; Torres, T.; Kostiainen, M. A., Phthalocyanine–Virus Nanofibers as Heterogeneous Catalysts for Continuous-Flow Photo-Oxidation Processes. *Adv. Mater.* **2019,** *31* (39), 1902582.
26. Makhseed, S.; Tuhl, A.; Samuel, J.; Zimcik, P.; Al-Awadi, N.; Novakova, V., New highly soluble phenoxy-substituted phthalocyanine and azaphthalocyanine derivatives: Synthesis, photochemical and photophysical studies and atypical aggregation behavior. *Dyes and Pigments* **2012,** *95* (2), 351-357.
27. Anaya-Plaza, E.; Joseph, J.; Bauroth, S.; Wagner, M.; Dolle, C.; Sekita, M.; Gröhn, F.; Spiecker, E.; Clark, T.; de la Escosura, A.; Guldi, D. M.; Torres, T., Synergy of Electrostatic and π–π Interactions in the Realization of Nanoscale Artificial Photosynthetic Model Systems. *Angewandte Chemie International Edition* **2020,** *59* (42), 18786-18794.
28. Wilkinson, F.; Helman, W. P.; Ross, A. B., Rate Constants for the Decay and Reactions of the Lowest Electronically Excited Singlet-State of Molecular-Oxygen in Solution - an Expanded and Revised Compilation. *Journal of Physical and Chemical Reference Data* **1995,** *24* (2), 663-1021.
29. Kupcho, K.; Shultz, J.; Hurst, R.; Hartnett, J.; Zhou, W.; Machleidt, T.; Grailer, J.; Worzella, T.; Riss, T.; Lazar, D.; Cali, J. J.; Niles, A., A real-time, bioluminescent annexin V assay for the assessment of apoptosis. *Apoptosis* **2019,** *24* (1), 184-197.
30. Machacek, M.; Demuth, J.; Cermak, P.; Vavreckova, M.; Hruba, L.; Jedlickova, A.; Kubat, P.; Simunek, T.; Novakova, V.; Zimcik, P., Tetra(3,4-pyrido)porphyrazines Caught in the Cationic Cage: Toward Nanomolar Active Photosensitizers. *Journal of Medicinal Chemistry* **2016,** *59* (20), 9443-9456.